Astrometric Measurements and Analysis of Double Star System BRT 376

Xinyue Wang
Stanford University Online High School, Stanford, CA
wxinyue@ohs.stanford.edu

Abstract

Using new telescope images and archival data, we investigated the positions and motions of the stars in double star system 06160-0745 BRT 376. We found that the two stars share nearly identical parallaxes and exhibit a low relative proper motion, suggesting they move together through space. Furthermore, their combined 3D velocity is less than the calculated escape velocity, indicating they are gravitationally bound rather than just physically near each other. These findings point to 06160-0745 BRT 376 being a true binary system. Future observations will help refine our understanding of its orbital path and further illuminate the nature of stars in close, interacting pairs.

1 Introduction

Double star systems exhibiting similar parallax and proper motion can be divided into two groups: physical doubles and binary stars. Physical doubles, which show nearly identical parallax and proper motion, indicate that the stars are spatially close and moving in unison. When such a physical double is gravitationally bound, it is classified as a binary system.

Physical doubles are valuable because they are likely to have a common origin, which allows researchers to analyze their behavior to infer aspects of galaxy evolution and to reconstruct events such as galaxy mergers. Conversely, binaries orbit a shared center of mass, enabling astronomers to determine the masses of both stars and, consequently, estimate their lifetimes. This paper investigates the likelihood of double star system 06160-0745 BRT 376's classification as either a physical double or binary system using inferences from archival data combined with new astrometric data.

The system 06160-0745 BRT 376 was selected from the Washington Double Star Catalog (WDS) based on the following criteria:

- Its right ascension (RA) must be between 5 and 13 hours, ensuring it is near the zenith during January and February, when the observations were made.
- Declination was not restricted since images were obtained through the Las Cumbres Observatory Global Telescope (LCOGT) network, which operates telescopes in both hemispheres.

- The secondary star must have a magnitude < 13, ensuring that both stars are sufficiently luminous to be clearly detected by a 0.35 m Delta Rho telescope.
- The brightness difference between the two stars should be less than 3 magnitudes, allowing them to be imaged simultaneously with the same exposure settings.
- The stars should have an angular separation between $5''$ and $15''$, ensuring that both components are distinctly resolved in the same image.
- The system must be listed as "physical" in the Stelle Doppie database, which indicates that the stars have similar parallaxes and proper motions.

For both the primary and secondary stars, BP-RP colors and G-filter magnitudes were obtained from Gaia Data Release 3 (DR3) [2, 3, 4]. The absolute magnitudes in the G filter were then calculated using Equation 1, which accounts for the effects of parallax on the magnitudes directly obtained from Gaia DR3.

$$\text{Absolute Gmag} = m + 5\left(\log p + 1\right) \tag{1}$$

Equation 1: Gaia G absolute magnitude (M) standardizes G-filter magnitude (m) by accounting for parallax (p).

Figure 1 was used to estimate spectral types by plotting Gaia BP-RP color and Gaia G absolute magnitude (Table 1). The Gaia BP-RP color on the x-axis is used as a proxy for surface temperature, while the Gaia G absolute magnitude on the y-axis is used as a proxy for luminosity. Spectral types were estimated by matching the star's position on Figure 1 to its spectral type marking. All stars of system 06160-0745 BRT 376 were found to be on the main sequence.

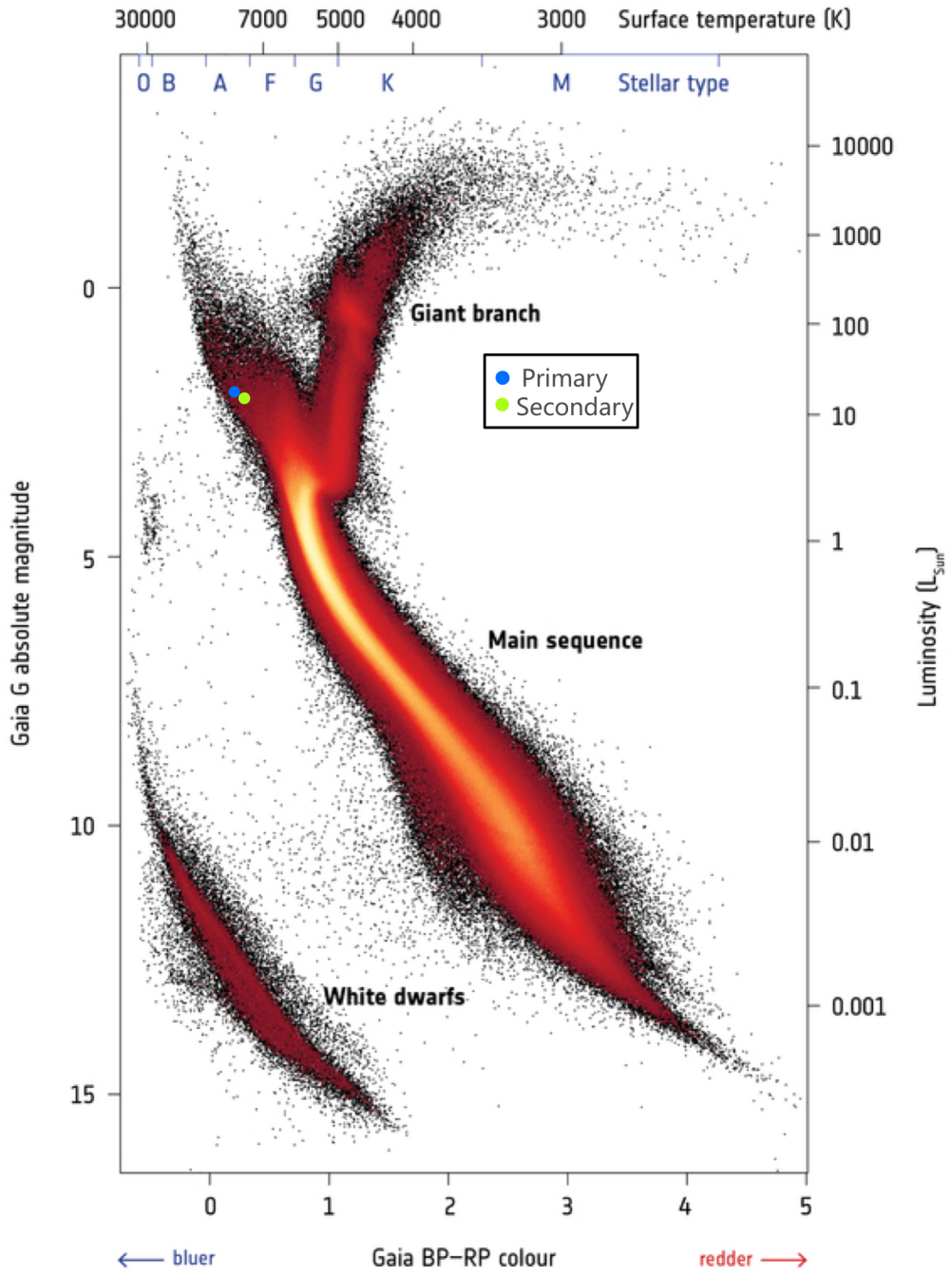

Figure 1: Gaia's Hertzsprung-Russell Diagram with primary (blue) and secondary (green) stars plotted according to BP-RP Color and Gaia G Absolute Magnitude [8].

Table 1: Colors and Magnitudes from Gaia DR3.

Star (Primary / Secondary)	Gaia BP-RP Color	Gaia G-Filter Magnitude (m)	Gaia G Absolute Magnitude (M)
Primary	0.24	9.44	2.05
Secondary	0.26	9.50	2.13

Table 2 summarizes the estimated spectral types derived from Figure 1, along with the corresponding mass estimates and the most recent measurements of position angle (PA) and separation (Sep) obtained from earlier studies listed in the SIMBAD database [7]. For every system, these spectral type estimates were verified against the University of Northern Iowa's catalog of spectral type characteristics to determine the masses [5].

Table 2: Basic Information on 06160-0745 BRT 376 with Spectral Type and Mass Estimates and Latest PA/Sep Measurements.

System	Star	Coordinates (HMS:DMS)	Spectral Type	Mass ($M_\odot$)	Latest PA/Sep Date	PA (°)	Sep (″)
06160-0745	BRT 376 Primary	06 15 57.81 -07 45 09.0	A3	1.9	2015.5 [8]	294.9	6.046
	BRT 376 Secondary	—	A4	1.8	—	—	—

2 Instruments

System 06160-0745 BRT 376 was imaged using telescopes from the Las Cumbres Observatory (LCOGT) robotic network [9]. The measurements were taken with the DeltaRho+QHY600 telescope-camera system, which features a 0.35 m aperture and a field of view of 1.9° × 1.2°, reduced to 30′ × 30′ in its default "central mode." The system was imaged using the Bessel-V (V) filter [1].

3 Measurements

Images were requested from the LCOGT network. Using AstroImageJ's (AIJ) multi-aperture photometry tool, measurements for position angle (PA) and separation (Sep) were made on all the requested images. A complete list of the individual observations is provided in Table 3, and Figure 2 displays an example of an AIJ measurement.

Table 3: Astronomical Measurements of Each Image.

Julian Date	Image / Value										
2024.019	1	2	3	4	5	6	7	8	9	10	11
PA (°)	294.30	294.94	295.04	294.20	295.37	294.33	294.47	294.25	294.68	294.59	294.39
Sep (″)	6.048	6.000	6.006	6.078	6.024	6.054	6.060	6.042	6.102	6.018	6.024

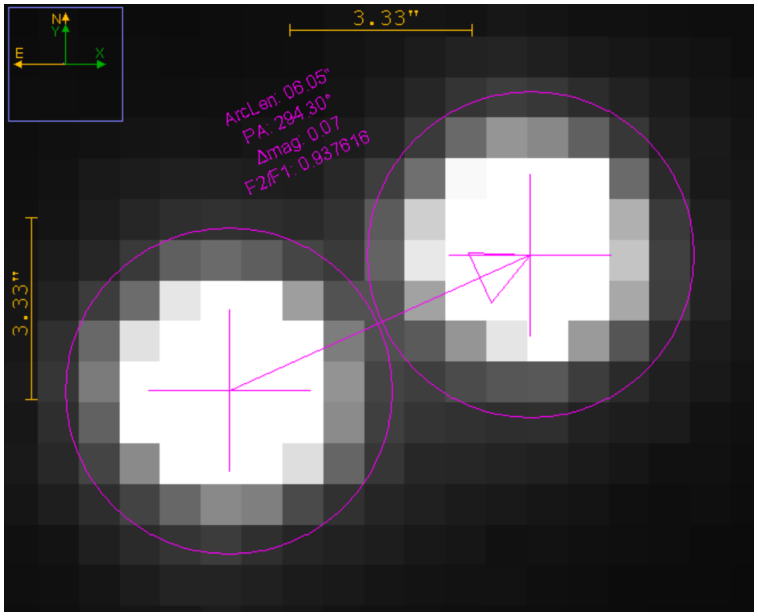

Figure 2: Screenshot of Image 1 taken from AIJ with multi-aperture photometry tool. System BRT 376 is pictured with a measured Sep of 6.048″ and PA of 294.30° in this particular image.

4 Results

Table 4 presents data from Gaia DR3, including parallax (with uncertainty), proper motions in RA and Dec, and the relative velocities for both stars in BRT 376. Using the Gaia DR3 proper motion components, we calculated the individual proper motion vector magnitudes for each star. The difference between these vectors gives the relative proper motion (PM) vector, whose magnitude is also listed in Table 4.

Table 4: Gaia DR3 Parallax and Proper Motion Measurements with Relative Proper Motions.

System	Star	Parallax (mas) ± Uncertainty	PM RA (mas/yr)	PM Dec (mas/yr)	Radial velocity (m/s)	Relative PM vector mag (mas/yr)
06160-0745 BRT 376	Primary	3.328 ± 0.018	-11.07993	-2.70812	89419	0.41
	Secondary	3.354 ± 0.017	-10.83261	-3.03914	-2073	0.04

The ratio of proper motion (rPM) in the final column is obtained by dividing the magnitude of the relative PM vector by the magnitude of the larger individual PM vector, as defined in Equation 2.

$$\text{rPM} = \frac{\|\mathbf{u} - \mathbf{v}\|}{\|\mathbf{v}\|} \tag{2}$$

Equation 2: The ratio of proper motion (rPM) is defined as the magnitude of the difference between the two stars' PM vectors (with v being the larger) divided by the magnitude of v.

A low rPM indicates that the secondary star's motion relative to the primary is small compared to the system's overall motion. This suggests that the stars are moving similarly

and are likely physically associated. For common proper motion (CPM) systems—the category indicating the strongest physical association—rPM values range from 0 to 0.2, which is the case for BRT 376 [10].

To assess gravitational binding, we compared the system's escape velocity with its relative 3D space velocity. The escape velocity is the minimum speed needed to overcome the gravitational pull of both stars, calculated using Equation 3 [11]:

$$v_e = \sqrt{\frac{2\,G\,(M_p + M_s)}{R}} \tag{3}$$

Equation 3: Escape velocity (v_e) is determined from the gravitational constant (G), the masses of the primary and secondary (M_p and M_s), and their separation (R).

Normally, R includes both the transverse and radial separations. However, due to overlapping parallax uncertainties (Table 4), we assume no radial separation and use the transverse distance as R. Equation 4 calculates the in-space transverse separation by combining the latest published separation (Table 1) with the system's parallax (Table 4).

$$R = \mathrm{Sep}_{\mathrm{pc}} \;=\; \frac{\mathrm{Sep}_{\mathrm{arcseconds}} \times \frac{1^\circ}{3600''} \times \frac{2\pi\,\mathrm{radians}}{360^\circ}}{\mathrm{Plx}''} \tag{4}$$

Equation 4: Computes the in-space transverse separation (R) from the latest separation (arcseconds) and parallax, yielding the physical separation in parsecs.

Another key metric in Table 5 is the relative 3D space velocity, which combines the relative transverse and radial velocities using the Euclidean norm. The relative transverse velocity is derived from the relative proper motion (from Table 4) using the small-angle tangent approximation to convert mas/year to m/s, while the relative radial velocity is the absolute difference in radial velocities between the primary and secondary stars (also from Table 4).

Table 5: Comparison of System Escape Velocity with Relative 3D Velocity.

System	System Escape Velocity (m/s)	Relative 3D Velocity (m/s)
06160-0745 BRT 376	1892.56	1087.85

If the relative 3D space velocity exceeds the system's escape velocity, the stars would have enough kinetic energy to overcome their mutual gravitational attraction and eventually separate. However, as shown in Table 5, the relative 3D velocity (1087.85 m/s) is below the escape velocity (1892.56 m/s), suggesting that system 06160-0745 BRT 376 is gravitationally bound.

5 Plots

Figures 3 and 4 display historical measurements of the secondary star's position in right ascension (RA) and declination (Dec) relative to the primary, which is fixed at the origin, for system 06160-0745 BRT 376. These positions were derived by converting historical PA and separation data into relative coordinates. In each plot, the Gaia DR3 measurement is marked by a red circle, while the measurement obtained in this study is indicated by a green "X." Figure 3 shows early observations (pre-1905) that exhibit a significant gap compared to more recent data, along with one likely outlier from 1979 that recorded an RA of $-5.75''$ [12]. In contrast, Figure 4 presents the data with the outlier removed and the axes adjusted accordingly. The plots were generated using the Python toolkit by Xinyue Wang [6].

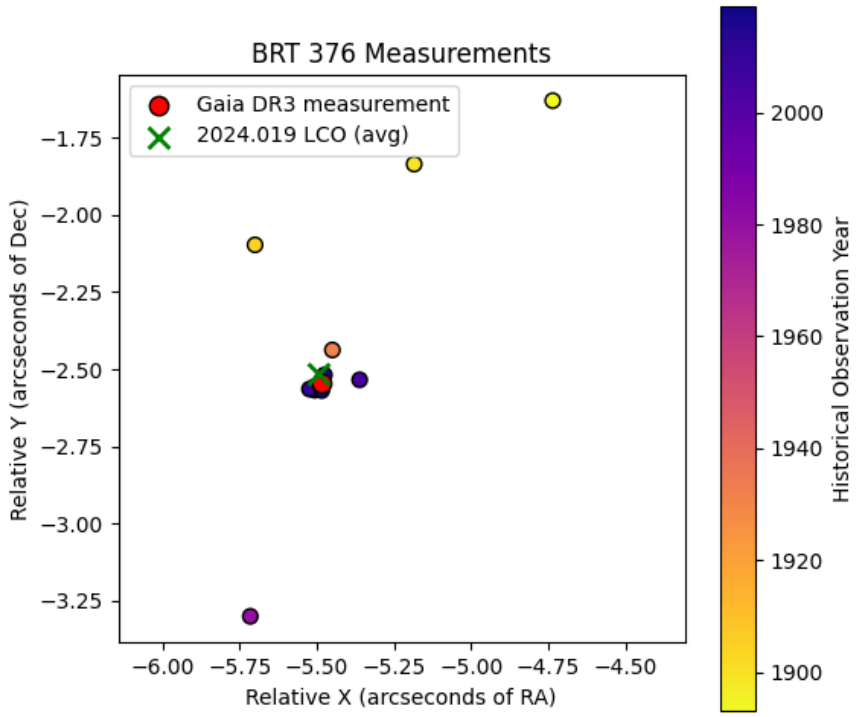

Figure 3: Relative position of the secondary star with respect to the primary of 06160-0745 BRT 376 (outlier included).

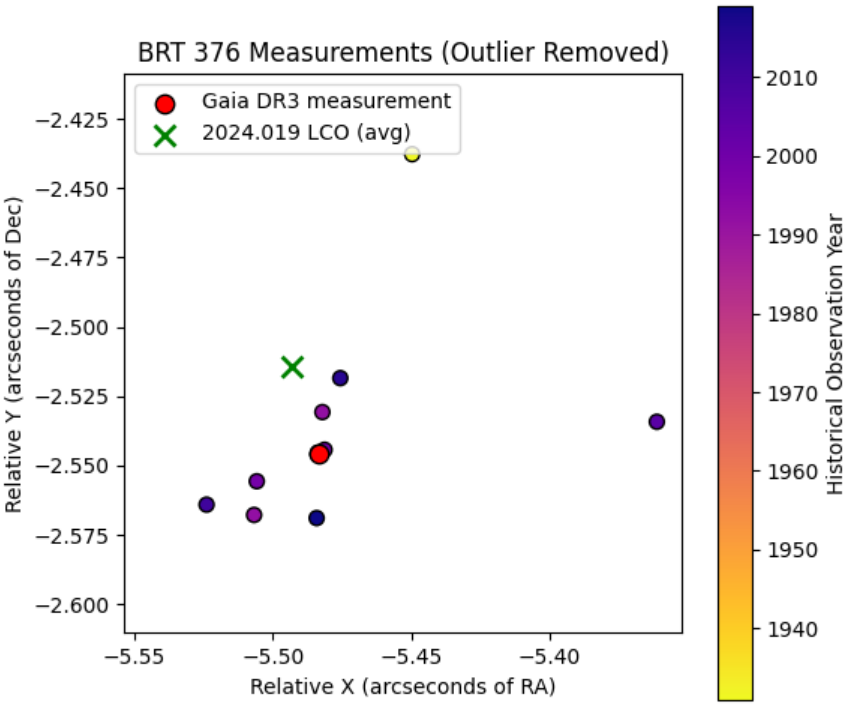

Figure 4: Figure 3 with outlier excluded.

While the earlier observations (shown in yellow) display a fair amount of scatter, the more recent data in Figure 4 suggest a possible trend in the secondary star's position over time. However, due to the limited number of observations since 2015, there is not enough evidence to confidently extend this trend into a broader relationship between the secondary and primary stars.

6 Discussion

The measurements presented here are broadly consistent with Gaia DR3 results, evidenced by the close agreement within 1″ between our new PA and separation values and those of Gaia. Figures 3 and 4 illustrate the historical positions of the secondary star relative to the primary, revealing scattered early observations and one apparent outlier from 1979. More recent data (post-2015) suggest a potential shift in the secondary star's relative position, though the small number of modern observations prevents a definitive conclusion regarding any orbital trend.

From a quantitative standpoint, three factors support the stars' physical association: (1) their overlapping parallax values imply negligible radial separation, (2) the ratio of proper motion (rPM < 0.2) falls well within the range for common proper motion [10], and (3) the relative 3D space velocity of 1087.85 m/s is below the escape velocity of 1892.56 m/s (Table 5). Consequently, the system 06160-0745 BRT 376 is likely gravitationally bound, suggesting it is a bona fide binary rather than a mere physical double. Ongoing and future observations will be valuable in confirming any orbital motion and further refining the system's dynamical parameters.

7 Conclusion

Our combined astrometric analysis and archival research strongly indicate that 06160-0745 BRT 376 is gravitationally bound. The system's overlapping parallaxes, low ratio of proper motion (rPM), and a relative 3D velocity below the escape velocity all point toward a bona fide binary rather than a mere physical double. Although recent observations hint at a potential orbital trend, additional data are needed to confirm and refine these findings. Continued monitoring will help clarify the system's exact orbital parameters and enhance our understanding of stellar evolution in close pairs.

Acknowledgements

I would like to extend my heartfelt thanks to team Schwarzschildren at Stanford University Online High School for their countless help and care. I am also deeply grateful to Kalée Tock, whose generous support made this research possible.

This work relied on several key resources and tools. Data were drawn from the Washington Double Star Catalog (maintained in the U.S. Naval Observatory) and the Stelledoppie database (`http://www.stelledoppie.it`), curated by Gianluca Sordiglioni. AstroImageJ software, developed by Karen Collins and John Kielkopf, was used for photometric measurements, and the SIMBAD database [7] at CDS in Strasbourg, France, provided supplementary information.

We also made use of data from the European Space Agency's Gaia mission, processed by the Gaia Data Processing and Analysis Consortium (DPAC), with support from national institutions under the Gaia Multilateral Agreement. Observations were obtained through the Planewave Delta Rho 350 + QHY600 CMOS camera systems at the Las Cumbres Observatory Global Telescope Network in Tenerife, Spain.

Additionally, the Stellarium planetarium was used for visualization, and Google Colab with the matplotlib library assisted in generating plots [6].

References

[1] Bessell, M. S. (1990). Publications of the Astronomical Society of the Pacific, 102, 1181–1199. `https://adsabs.harvard.edu/full/1990PASP..102.1181B`

[2] Gaia Collaboration, C. Babusiaux, C. Fabricius, S. Khanna, et al. (2023) Gaia Data Release 3. Catalogue validation. A&A 674, pp. A32. `https://arxiv.org/abs/2206.05989`

[3] Gaia Collaboration, T. Prusti, J.H.J. de Bruijne, et al. (2016b). The Gaia mission. A&A 595, A1. `https://www.aanda.org/articles/aa/full_html/2016/11/aa29272-16/aa29272-16.html`

[4] Gaia Collaboration, A. Vallenari, A. G. A. Brown, et al. (2023j) Gaia Data Release 3. Summary of the content and survey properties. A&A 674, pp. A1. `https://arxiv.org/abs/2208.00211`

[5] Morgan, Siobahn (2023). Spectral Type Characteristics. Retrieved Feb, 2025 from https://sites.uni.edu/morgans/astro/course/Notes/section2/spectralmasses.html

[6] Wang, Xinyue. (2025). A Python Toolkit for Plotting Double Star Observations with 1:1 Aspect Ratio. https://arxiv.org/abs/2502.13340

[7] Wenger, M. et al. (2000). The SIMBAD astronomical database. The CDS reference database for astronomical objects. Astronomy and Astrophysics Supplement 143, pp. 9–22. Retrieved from astro-ph/0002110 [astro-ph].

[8] Gaia Collaboration et al. (2018) Gaia Data Release 2. Summary of the contents and survey properties. Astronomy & Astrophysics, 616, A10. DOI: https://doi.org/10.1051/0004-6361/201832843

[9] Brown, T. M. et al. (2013). Las Cumbres Observatory Global Telescope Network. Publications of the Astronomical Society of the Pacific, 125(931), 1031–1055. Retrieved from https://iopscience.iop.org/article/10.1086/673168/meta

[10] Harshaw, Richard (2016). CCD Measurements of 141 Proper Motion Stars: The Autumn 2015 Observing Program at the Brilliant Sky Observatory, Part 3. Journal of Double Star Observations, 12(4), 394–399. Retrieved from http://www.jdso.org/volume12/number4/Harshaw_394_399.pdf

[11] Bonifacio, B., C. Marchetti, R. Caputo, et al. (2020). Measurements of Neglected Double Stars. Journal of Double Star Observations, 16(5), 411–423. Retrieved from http://www.jdso.org/volume16/number5/Bonifacio_411_423.pdf

[12] Tobal, T. & Planas, J. (2003). OAG General Catalog of 10,000 Visual Double Stars Measurements 1970–2003 (J2000.0), Vol. I & II. OAG Publications: Measurements of Double Stars in USNO/WDS, OAG General Catalog.